

# Therapeutic function of a novel rat induced pluripotent stem cell line in a 6-OHDA-induced rat model of Parkinson's disease

JIAJIA XU<sup>1\*</sup>, YANGYANG LI<sup>1\*</sup>, HUAN ZHU<sup>2\*</sup>, WENYU WU<sup>1</sup>, YUMENG LIU<sup>1</sup>,  
YU GUO<sup>3</sup>, WEIJUN GUAN<sup>4</sup>, CHANGQING LIU<sup>1</sup> and CAIYUN MA<sup>1,4</sup>

<sup>1</sup>School of Life Sciences, Bengbu Medical College, Bengbu, Anhui 233000; <sup>2</sup>Department of Blood Transfusion, The Affiliated Hospital of Yangzhou University, Yangzhou, Jiangsu 225001; <sup>3</sup>School of Laboratory Medicine, Bengbu Medical College, Bengbu, Anhui 233000; <sup>4</sup>National Germplasm Resource Center for Domestic Animals, Institute of Beijing Animal and Veterinary Science, Chinese Academy of Agricultural Science, Beijing 100193, P.R. China

Received June 3, 2022; Accepted October 4, 2022

DOI: 10.3892/ijmm.2022.5196

**Abstract.** Parkinson's disease (PD) is a progressive neurodegenerative movement disorder of the central nervous system that results from the loss of dopaminergic (DA) nigral neurons. Induced pluripotent stem cells (iPSCs) have shown potential for cell transplantation treatment of neurodegenerative disorders. In the present study, the small molecules CHIR99021 and RepSox (CR) significantly facilitated reprogramming and enhanced the efficiency of GFP<sup>+</sup>/iPS-like colonies [rat iPSCs induced by OCT3/4, Sox2, Klf4, c-Myc, Nanog and Lin28 + CR (RiPSCs-6F/CR)] generation by ~4.0-fold during lentivirus-mediated reprogramming of six transcription factors in rat embryonic fibroblasts. The generation of iPSCs was detected by reverse transcription-PCR, immunofluorescence and western blot analysis. Subsequently, RiPSCs-6F/CR were stereotactically transplanted into the right medial forebrain bundle (MFB) of 6-hydroxydopamine-lesioned rats with PD. The transplanted RiPSCs-6F/CR survived and functioned in the MFB of rats with PD for ≥20 weeks, and significantly improved functional restoration from their PD-related behavioral defects. Furthermore, the grafted RiPSCs-6F/CR could migrate and differentiate into various neurocytes *in vivo*, including  $\gamma$  aminobutyric acid-ergic, DA neurons and glial cells. In conclusion, the present study confirmed that RiPSCs-6F/CR induced by small molecules could be used as potential donor material for neural grafting to remodel basal ganglia circuitry in neurodegenerative diseases.

## Introduction

Parkinson's disease (PD) is the second most common neurodegenerative disease after Alzheimer's disease, affecting 1-3% of the population >60 years old worldwide (1). The main pathology of PD is the progressive loss of dopaminergic (DA) neurons in the substantia nigra and formation of  $\alpha$ -synuclein-containing Lewy bodies (2,3). Early PD responds well to DA drugs, such as L-3,4-dihydroxyphenylalanine, dopamine agonists, and monoamine oxidase and catechol-O-methyl-transferase inhibitors (4). However, over time, these drugs begin to lose their effectiveness and cause side effects, including movement disorders and neuropsychiatric complications (5,6). At present, there are two main surgical methods that can be used as an effective adjuvant therapy to drug treatment: Nucleus lesioning surgery and deep brain stimulation (DBS) (3). Nucleus lesioning is irreversible damage to the brain nuclei, such as the globus pallidus internus and the subthalamic nucleus (STN), accompanied by serious complications including hemiparesis, visual disturbances and permanent speech deficits, whereas DBS targets the STN and medial globus pallidus nucleus (7,8). However, DBS exhibits complications, such as tolerance and electrode displacement, and is associated with a high cost; therefore, it is not a popular approach (9-11).

In previous years, stem cell transplantation therapies have been considered a potential method for the treatment of PD (12,13). In 2006, induced pluripotent stem cells (iPSCs) reprogrammed from somatic cells became a hot topic in research (14,15). Notably, iPSC technology can efficiently generate patient- and disease-specific PSC lines, which can then differentiate into any desired cell type, potentially solving a major problem in stem cell therapy (14,16-19). Given the inherent self-renewal capacity, pluripotency and relatively low immunogenicity of iPSCs (20), they provide a promising patient-derived cell resource for human genetic disease modeling and toxicity studies, thereby reducing the overall cost and associated risks of drug development and clinical trials (21-23). Moreover, functional midbrain DA progenitors and neural progenitor cells (NPCs) derived from iPSCs could survive and restore motor function in the treatment of neurodegenerative diseases (24-26). Furthermore,

---

*Correspondence to:* Dr Changqing Liu or Dr Caiyun Ma, School of Life Sciences, Bengbu Medical College, 2600 Donghai Avenue, Bengbu, Anhui 233000, P.R. China  
E-mail: lcq7813@bbmc.edu.cn  
E-mail: caiyun\_ma@bbmc.edu.cn

\*Contributed equally

**Key words:** Parkinson's disease, rat induced pluripotent stem cells, cell reprogramming, neural transplantation, small molecules

long-term survival and function of midbrain-like DA neurons derived from autologous human iPSCs have been reported in a non-human primate model of PD (27,28).

The present study used a lentivirus encoding six reprogramming factors to reprogram rat embryonic fibroblasts (REFs) to generate pluripotent cells *in vitro*, and the small molecules CHIR99021 and RepSox (CR) significantly enhanced the generation of iPSC colonies. Subsequently, the novel rat iPSCs were directly transplanted into the medial forebrain bundle (MFB) of rats with PD to investigate the functional effects of the transplanted cells *in vivo*, which provided experimental evidence for studying the pathogenesis of PD and identifying the potential of iPSCs for neural transplantation.

## Materials and methods

**Animals.** A total of 48 specific-pathogen-free, 8-week-old, healthy male Sprague-Dawley (SD) rats (weight ~200 g) and two pregnant SD rats (weight ~350 g) were provided by the Experimental Animal Center of Anhui Medical University (Hefei, China). The rats were maintained in groups of five per cage under a 12-h light/dark cycle, the relative humidity was controlled at 40-70% and the temperature was controlled at 23±2°C, with *ad libitum* access to food and water. During the experimental period, if any rat started to show signs of immobility, a huddled posture, inability to eat, ruffled fur or self-mutilation, they were immediately sacrificed. In addition, animals were euthanized to prevent further suffering if they were unable to stand or displayed agonal breathing, severe muscular atrophy, severe ulcers or uncontrolled bleeding. The animals were anesthetized with an intraperitoneal injection of 3% sodium pentobarbital (50 mg/kg; Merck KGaA) before 6-OHDA injection, cell transplantation and perfusion. Subsequently, the rats with unsuccessful modeling were euthanized by cervical dislocation under anesthesia or were injected with an overdose of sodium pentobarbital (150 mg/kg) for euthanasia. In addition, complete cardiac and respiratory arrest were observed to verify animal death. All of the experimental animal procedures were approved by the Institutional Animal Care and Use Committee of Bengbu Medical College (Bengbu, China; approval no. 2020-025).

**Culture of REFs.** Primary REFs were mechanically isolated and cultured from 16 embryonic day (E)16-18 rat embryos as previously described (29). Briefly, uteri were isolated from two E16-18 pregnant SD rats following deep anesthesia via a subcutaneous injection of 3% sodium pentobarbital (50 mg/kg), as aforementioned. The head, limbs, visceral tissues and gonads were removed from the isolated embryos. The remaining body parts were minced and trypsinized using 0.1 mM trypsin/1 mM EDTA solution for 20 min at 37°C. Cells in the supernatant were collected by centrifugation (200 × g for 5 min at 4°C), resuspended in fresh high-glucose Dulbecco's modified Eagle's medium (H-DMEM; Gibco; Thermo Fisher Scientific, Inc.) supplemented with 10% FBS (Gibco; Thermo Fisher Scientific, Inc.), 1% GlutaMax (Thermo Fisher Scientific, Inc.), 1% non-essential amino acid (NEAA), 100 U/ml penicillin and 0.1 mg/ml streptomycin, and cultured at 37°C in a 5% CO<sub>2</sub> incubator. In the present study, REFs within five passages were used to avoid replicative senescence and genetic characteristic

instability. The expression of fibroblast-specific marker genes (*CD34*, *COL1A1* and *S100a4*) and epithelial cell-specific marker genes (*CDH1* and *MUC1*) were analyzed by reverse transcription-PCR (RT-PCR) as described previously (30-32). The expression of fibroblast-specific markers, including CD34 (1:500; Affinity Biosciences) and Vimentin (1:500; BLOSS) were also detected by immunofluorescence (IF) as described previously (31-35).

**Plasmid construction and lentivirus production using second-generation lentivirus system.** The cDNA of six reprogramming factors, namely OCT3/4, Sox2, Klf4, c-Myc, Nanog and Lin28 (OSKMNL), were inserted downstream of the EF-1 $\alpha$  promoter and upstream of IRES-EFGP in the lentiviral vector to construct six Lenti-EF-1 $\alpha$ -X-IRES-EFGP lentivirus plasmids, (SiDan Sai Biotechnology Co., Ltd.). The day before transfection, 293T cells (gifted by Dr Liang Meng, Bengbu Medical College) were seeded at 10<sup>7</sup> cells per gelatin-coated T75 flask. The following day, six lentiviral plasmids (10  $\mu$ g) were co-transfected into 293T cells with pSVSG (5  $\mu$ g) and pCMV-dR8.91 (7.5  $\mu$ g) (both from Addgene, Inc.) using 56  $\mu$ l FuGENE<sup>®</sup> 6 Transfection Reagent (Roche Diagnostics) according to the manufacturer's protocols. Cells were then incubated overnight at 37°C in an atmosphere containing 5% CO<sub>2</sub>. At 24 h post-transfection, the medium was replaced. After 48 and 96 h, the virus-containing supernatants were collected and filtered through a 0.45- $\mu$ m polyvinylidene fluoride (PVDF) filter. Titers of six lentiviruses were then determined according to the proportion of green fluorescence-emitting cells to total 293T transfected cells.

**Reprogramming rat fibroblasts to iPSCs.** For reprogramming, the initial REFs from a male rat embryo at passage 3 (P3) were co-transduced with six lentiviruses carrying six reprogramming factors (OSKMNL) and GFP-tagged protein at day 0 with a multiplicity of infection of 10 for each lentivirus (10 viral particles/cell) and supplemented with 10  $\mu$ g/ml polybrene. Cells were incubated in the virus/polybrene-containing supernatants for 24 h at 37°C, and then the medium was changed to fresh complete medium (H-DMEM containing 10% FBS). At day 2 post-transduction, REFs were re-plated on an irradiated OriCell<sup>®</sup> ICR mouse embryonic fibroblast feeder layer (Cyagen Biosciences, Inc.). The following day, the culture medium was replaced with DMEM/F-12 supplemented with 10% KnockOut Serum Replacement (Gibco; Thermo Fisher Scientific, Inc.), 0.1 mM  $\beta$ -mercaptoethanol, 1% NEAA, 2 mM L-glutamine, 100 U/ml penicillin and 0.1 mg/ml streptomycin, which was further supplemented with 3  $\mu$ M CHIR99021 (Sigma-Aldrich; Merck KGaA), 1  $\mu$ M RepSox (Selleck Chemicals) and 15 ng/ml fibroblast growth factor 2 (R&D Systems, Inc.) on day 4 (36,37). The GFP<sup>+</sup>/iPS-like colonies [rat iPSCs induced by OCT3/4, Sox2, Klf4, c-Myc, Nanog and Lin28 + CR (RiPSCs-6F/CR)] were mechanically picked 20-30 days after viral transduction and re-cultured on feeder layers. In addition, REFs treated with empty lentiviral particles and CR were used as a negative control and original REFs were used as blank control. The RiPSCs-6F/CR were analyzed for chromosomal alterations by G-band karyotype analysis at P6. The cells (~1.0×10<sup>6</sup> cells) were treated with 1.0 g/l colchicine solution and were then treated with 0.025 M KCl hypotonic

solution for 30 min in a 37°C water bath and with carnoy fixative (methanol:glacial acetic acid, 3:1) in a 37°C water bath for 5 min. Giemsa staining was performed following standard method (38). Subsequently, the well-spread chromosome metaphases were observed under an oil immersion objective (inverted fluorescence microscope; magnification, x1,000) and analyzed with VideoTesT-Karyo 3.1 software (NatureGene Corp.).

**Alkaline phosphatase (AP) staining and IF.** To detect AP activity, the compact cell colonies formed from REFs were washed with PBS three times and stained with an AP kit (cat. no. C3206; Beyotime Institute of Biotechnology) according to the manufacturer's protocol. The full and bright GFP-positive colonies were selected under a fluorescence microscope. To biologically characterize RiPSCs-6F/CR, cells seeded on coverslips were fixed with 4% (w/v) paraformaldehyde (PFA) for 18 min, permeabilized with 0.2% Triton X-100 for 8 min, and blocked with 10% goat serum and 10% donkey serum (both from Jackson ImmunoResearch Laboratories, Inc.) at room temperature for 1 h. Subsequently, the cells were incubated for 12 h at 4°C with the following primary antibodies against pluripotency markers: Anti-OCT4 (1:200; Abcam), anti-Nanog (1:300) and anti-Sox2 (1:400; both from Cell Signaling Technology, Inc.). The samples were then incubated with a cyanine 3 (Cy3) dye-conjugated secondary antibody (1:1,000; cat. no. 711-165-152; Jackson ImmunoResearch Laboratories, Inc.) for 1 h at room temperature. The cell nuclei were counterstained with DAPI (Thermo Fisher Scientific, Inc.) for 15 min at room temperature. Finally, the coverslips were mounted with ProLong™ Gold Antifade Mountant (Invitrogen; Thermo Fisher Scientific, Inc.) and observed under an inverted fluorescence microscope (Guangzhou Micro-shot Technology Co., Ltd.) (1,36).

#### Analyses of pluripotency markers for RiPSCs-6F/CR

**Flow cytometry.** Following digestion of RiPSCs-6F/CR with 0.25% trypsin to prepare a single-cell suspension and fixing with 4% (w/v) PFA for 30 min, the cells were permeabilized with 0.2% Triton X-100 for 10 min and blocked with 1% BSA (Sigma-Aldrich; Merck KGaA) + 10% donkey serum at room temperature for 1 h. Subsequently, the cells were incubated overnight at 4°C with the following primary antibodies against pluripotency markers: Anti-OCT4 (1:200; Abcam) and anti-Sox2 (1:400; Cell Signaling Technology, Inc.), and then with a Cy3 dye-conjugated secondary antibody (1:1,000; cat. no. 711-165-152, Jackson ImmunoResearch Laboratories, Inc.) for 1 h at room temperature. Finally, the cells were analyzed immediately by flow cytometry (DxP Athena 1L-3L; Cytex Biosciences) using FlowJo CE V10.1 software (FlowJo LLC).

**RT-PCR.** Total RNA was extracted from the cells using TRIzol® reagent (Invitrogen; Thermo Fisher Scientific, Inc.) and reverse transcribed into cDNA using PrimeScript™ RT Reagent Kit (Perfect Real time) (Takara Biotechnology Co., Ltd.) with the following parameters: 37°C for 15 min, 85°C for 5 sec and finally 4°C for 5 min. RT-PCR was carried out using TB Green Premix Ex Taq II (Takara Biotechnology Co., Ltd.) with a QuantStudio™ 6 Flex thermocycler (Applied Biosystems; Thermo Fisher Scientific, Inc.). The thermocycling

conditions were as follows: Initial denaturation at 95°C for 30 sec, followed by 40 cycles of denaturation at 95°C for 10 sec and at 60°C for 20 sec. The amplified fragments were visualized by 1% agarose gel electrophoresis and stained with Gel-Red (cat. no. D0140; Beyotime Institute of Biotechnology, Inc.), and GAPDH was used as the internal control. The primers were synthesized by Sangon Biotech Co, Ltd., and their sequences are shown in Table SI.

**Western blotting.** Total proteins were extracted from the REFs and RiPSCs-6F/CR using the total protein extraction kit (cat. no. P0028; Beyotime Institute of Biotechnology) and quantified using a BCA protein assay kit (cat. no. P0010; Beyotime Institute of Biotechnology). Equivalent quantities of protein (40 µg/sample) were separated by SDS-PAGE on 10% gels and electroblotted onto PVDF membranes (0.45 µM; MilliporeSigma). The membranes were blocked with 5% skimmed milk powder diluted in TBS-0.05% Tween at room temperature for 1 h and immunoblotted overnight at 4°C with the following primary antibodies: Rabbit anti-OCT4 (1:200; Abcam), rabbit anti-Nanog (1:300), rabbit anti-Sox2 (1:500; both from Cell Signaling Technology, Inc.) and mouse anti-β-actin (1:1,000; Affinity Biosciences). Subsequently, the membranes were incubated with a HRP-labeled secondary antibody (1:5,000; cat. no. 111-035-003; Jackson ImmunoResearch Laboratories, Inc.) for 1 h at room temperature. The protein bands were then visualized using Clarity Western ECL Substrate (Bio-Rad Laboratories, Inc.) and were semi-quantified using Quantity One software version 1-D (Bio-Rad Laboratories, Inc.).

#### 6-Hydroxydopamine (6-OHDA)-lesioned rat model of PD.

Healthy adult SD rats were deeply anesthetized with an intraperitoneal injection of pentobarbital sodium (50 mg/kg) and fixed on a brain stereotaxic apparatus (Reward Life Technology Co., Ltd.). The anesthetized rats were unilaterally infused with 8 µl 6-OHDA solution (5 mg/ml, dissolved in 0.2% ascorbate saline; Sigma-Aldrich; Merck KGaA) into the right MFB (n=36) at a rate of 0.5 µl/min at the following two coordinates related to the bregma: Anteroposterior (AP)=-4.4, mediolateral (ML)=-1.0 mm, dorsoventral (DV)=-7.8; and AP=-4.0, ML=-0.8 mm, DV=-8.0, and the needle was left in place for an additional 8 min before retraction. The skin incision was then closed with stainless steel wound clips.

#### Behavioral detection of rat models of PD

**Sniff test.** A total of 2 weeks after injection of 6-OHDA, the rats underwent a sniff test. Rats with PD usually sniff an unfamiliar environment standing on the ground, with movements of vibrissae and the head tilted upwards (39).

**Apomorphine (APO)-induced rotation experiment.** At week 2 after 6-OHDA unilateral injection, an intraperitoneal injection of APO (0.5 mg/kg; Sigma-Aldrich; Merck KGaA) was used to induce rotational behavior contralateral to the lesion side. A rotational speed of ≥210 revolutions/30 min was considered as the criterion for successful modeling of rats with PD. The experiment was performed at 4, 8, 12, 20 and 24 weeks after cell transplantation.

**Rotarod test.** A total of three rats were placed on the three channels of a rotarod test apparatus (SANS, Biotechnology Co., Ltd.). The rats placed on the rod synchronously were

detected simultaneously to assess motor coordination. The test was processed at a constant speed of 300 rpm for 1,800 sec, and each animal underwent three trials. Each trial was automatically paused, and the time it took for the rat to fall off the rod or run for 1,800 sec was recorded. If a rat fell within 10 sec, three repetitions of the experiment would be performed. The experiment was performed at 4, 8, 12, 20 and 24 weeks after cell transplantation.

*Open-field assay.* Each rat was placed into the central grid of the open-field instrument (Noldus Information Tech, Inc.), and the surrounding curtains were quickly drawn. The Ethovision XT 10.1S system of open-field instrument (Noldus Information Technology BV) automatically captured the track of the rat within 5 min and analyzed its stay in the central grid and the total distance of movement. Zone heatmaps were obtained by tracing the path of the rat in the open field. The experiment was performed at 4, 8, 12, 20 and 24 weeks after cell transplantation.

*Transplantation of RiPSCs-6F/CR into the right MFB of rats with PD.* A total of 2 weeks after 6-OHDA injection, RiPSCs-6F/CR and RiPSCs-6F (rat iPSCs induced by OSKMNL only) were resuspended in serum-free H-DMEM at a cell density of  $1.25 \times 10^7$  cells/ml and stereotactically transplanted into the right MFB of model rats with PD according to the same two stereotaxic coordinates as the PD model. At each site, an aliquot (8  $\mu$ l) of cell suspension including  $1.0 \times 10^5$  cells was injected into each rat with PD using a microsyringe at a rate of 0.5  $\mu$ l/min. The rats were divided into the following four groups: i) Control group containing 12 healthy rats, which were injected with 8  $\mu$ l saline. A total of 30 model rats with PD (out of the initial 36 rats used for PD modelling, 83.3% success rate) were divided randomly into three groups, including a ii) vehicle group containing 12 PD model rats, which were injected with 8  $\mu$ l H-DMEM; iii) a RiPSCs-6F/CR group containing 12 PD model rats injected with  $1.0 \times 10^5$  RiPSCs-6F/CR; and iv) a RiPSCs-6F group containing six PD model rats injected with  $1.0 \times 10^5$  RiPSCs-6F.

Behavioral analysis was performed on each group at 4, 8, 12, 20 and 24 weeks after cell transplantation. In total, two rats from each group were perfused, and coronal sections of the perfused brains were used for IF detection at 8 and 20 weeks after cell transplantation. On week 12, two rats from each group were perfused for hematoxylin and eosin (H&E) staining and tyrosine hydroxylase (TH)-3,3'-diaminobenzidine (DAB) detection by immunohistochemical analysis. Each test requiring sacrifice of experimental animals was repeated only once, i.e. two rats were sacrificed per test. And, the remaining six rats from each of the three groups were used for long-term monitoring of behavioral changes.

*Histology and immunohistochemistry (IHC).* Rats were deeply anesthetized with intraperitoneal injections of 3% pentobarbital sodium (50 mg/kg), and then transcardially perfused with 0.9% NaCl followed by 4% PFA. During PFA perfusion, the limbs of the rats twitched continuously and became rigid, and the liver and brain became white, thus confirming successful perfusion and rat euthanasia. The brain was collected and fixed in 4% paraformaldehyde at 4°C for 6 h, after which the brain tissue was transferred into 25%

sucrose solution until it sank to the bottom at 4°C. The brain tissue was then incubated at -80°C overnight. Subsequently, the perfused brains were embedded using OCT embedding medium (Sakura Finetek USA, Inc.) and serial coronal sections (12  $\mu$ m) were cut using a cryostat (CM-1850; Leica Microsystems, Inc.), mounted on gelatin-coated glass slides and frozen at -20°C. Subsequently, the sections were permeabilized with 0.2% Triton X-100 for 8 min at room temperature, and blocked with 10% goat serum and 10% donkey serum at room temperature for 1 h. The sections were then subjected to double IF staining using an anti-GFP antibody (1:200) and the following nerve-specific labeling antibodies: Anti- $\beta$ III tubulin (TUJ1; 1:500), anti-Nestin (1:200), anti-TH (1:300), anti-paired box protein 6 (PAX6; 1:200), anti-synaptophysin (SYN; 1:1,000; all from Abcam), anti- $\gamma$  aminobutyric acid (GABA; 1:300; Sigma-Aldrich; Merck KGaA), anti-Sox2 (1:500), anti-postsynaptic density protein 95 (PSD95; 1:300; both from Cell Signaling Technology, Inc.) and anti-glial fibrillary acidic protein (GFAP; 1:300; Neuromics). Details of all the primary antibodies used in the current study are listed in Table SII. Subsequently, the samples were incubated with appropriate Alexa Fluor 488 (1:500; cat. no. A-21202; Invitrogen; Thermo Fisher Scientific, Inc.) and Cy3-conjugated (1:1,000; cat. no. 711-165-152; Jackson ImmunoResearch Laboratories, Inc.) secondary antibodies, followed by incubation with DAPI for nuclear staining. Images were obtained using a multiphoton laser scanning confocal microscope (FV-1200MPE SHARE; Olympus Corporation).

Perfused brains collected at 12 weeks after cell transplantation were paraffin embedded and cut into 30- $\mu$ m sections. Antigen retrieval was performed using citric acid antigen retrieval buffer (cat. no. G1202; pH 6.0; Wuhan Servicebio Technology Co., Ltd.) in a microwave oven. To block endogenous peroxidase activity, the sections were incubated in 3% hydrogen peroxide (Disinfection Technology Co. Ltd.) at room temperature in the dark for 25 min. Subsequently, sections were blocked with 3% BSA (G5001; Wuhan Servicebio Technology Co., Ltd.) for 30 min at room temperature. The sections were then incubated with an anti-TH (1:300; cat. no. ab112; Abcam) antibody for 1 h at room temperature. Subsequently, the sections were washed three times with Dulbecco's PBS, and were incubated with a HRP-conjugated goat anti-rabbit secondary antibody (1:1,000; cat. no. 111-035-003; Jackson Immunoresearch Laboratories, Inc.) for 1 h at room temperature. The sections were then stained with 3,3'-diaminobenzidine tetrahydrochloride solution (cat. no. G1211; Wuhan Servicebio Technology Co., Ltd.) at room temperature; the color developing time (1-10 min) was controlled under the microscope.

Additionally, histopathological examination of 3- $\mu$ m paraffin-embedded sections was routinely performed using a H&E staining kit (Wuhan Servicebio Technology Co., Ltd.). The paraffin-embedded sections were first dewaxed with xylene, then dehydrated with increasing ethanol concentrations, washed with PBS and stained with H&E staining solution at room temperature for 5 min. The survival and number of TH<sup>+</sup> cells obtained from TH-DAB and H&E staining were calculated by whole brain scanning using a Nikon Imaging System (DS-U3; Nikon Corporation) and CaseViewer 2.0

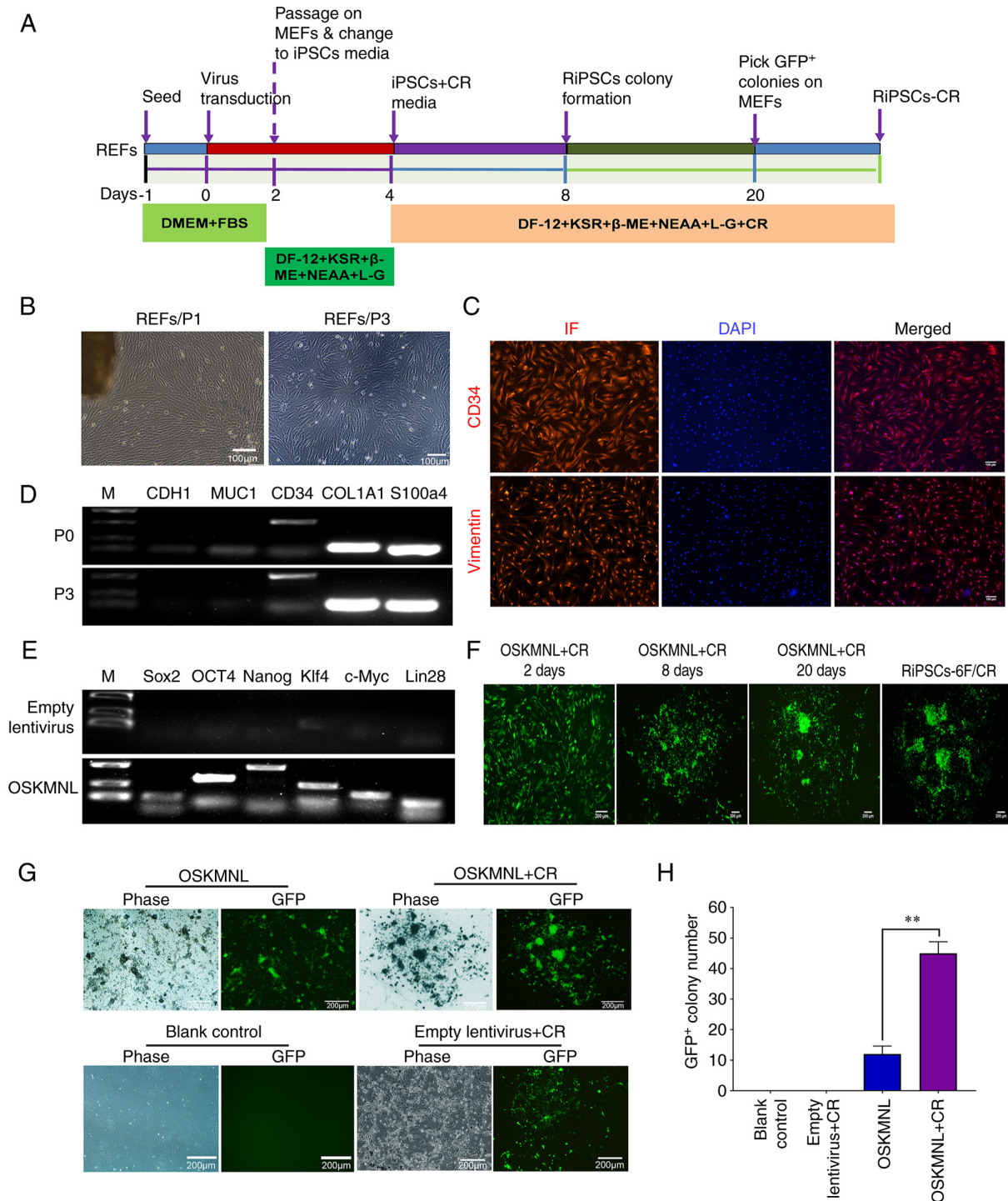


**Figure 1.** Induction and characterization of RiPSCs-6F/CR generated from REFs. (A) Schematic representation of the OSKMNL-CR transduction reprogramming protocol. (B) Morphology of REFs at P1 and P3. Fibroblast-like cells could be seen migrating from the tissue pieces in the P1 image. (C) REFs expressed fibroblast markers CD34 and Vimentin, as observed by IF staining (scale bars, 100  $\mu$ m). (D) Expression of fibroblast- and epithelial-specific marker genes was detected by reverse transcription-PCR. (E) All OSKMNL genes were overexpressed 3 days after infection of REFs with OSKMNL-expressing lentiviral particles. According to the size of the PCR amplification fragment, the upper bands were determined as the target bands. The bands below are primer dimers of PCR amplification, which may be attributed to the low annealing temperature and high primer concentration. (F) Cell morphological changes throughout the induction process. (G) GFP<sup>+</sup>/iPS-like colonies were induced by OSKMNL and OSKMNL + CR; CR markedly promoted the efficiency of GFP<sup>+</sup>/iPS-like colonies generation. (H) Statistical analysis of the number of GFP<sup>+</sup> clones. \*\* $P < 0.01$  vs. OSKMNL+CR. RiPSCs-6F/CR, rat iPSCs induced by OSKMNL + CR; REFs, rat embryonic fibroblasts; MEFs, mouse embryonic fibroblasts; iPSCs, induced pluripotent stem cells; OSKMNL, OCT3/4, Sox2, Klf4, c-Myc, Nanog and Lin28; DF-12, DMEM/F-12; DMEM, Dulbecco's modified Eagle's medium; KSR, KnockOut Serum Replacement;  $\beta$ -ME,  $\beta$ -mercaptoethanol; NEAA, non-essential amino acid; L-G, L-glutamine; CR, CHIR99021 and RepSox; P, passage; IF, immunofluorescence.

software (3DHISTECH, Ltd.). The number of TH<sup>+</sup> cells in three randomly selected fields was counted using ImageJ software (1.51r; National Institutes of Health).

**Statistical analysis.** All quantitative data are presented as the mean  $\pm$  standard error of the mean from at least three independent experiments. Statistical comparisons between two

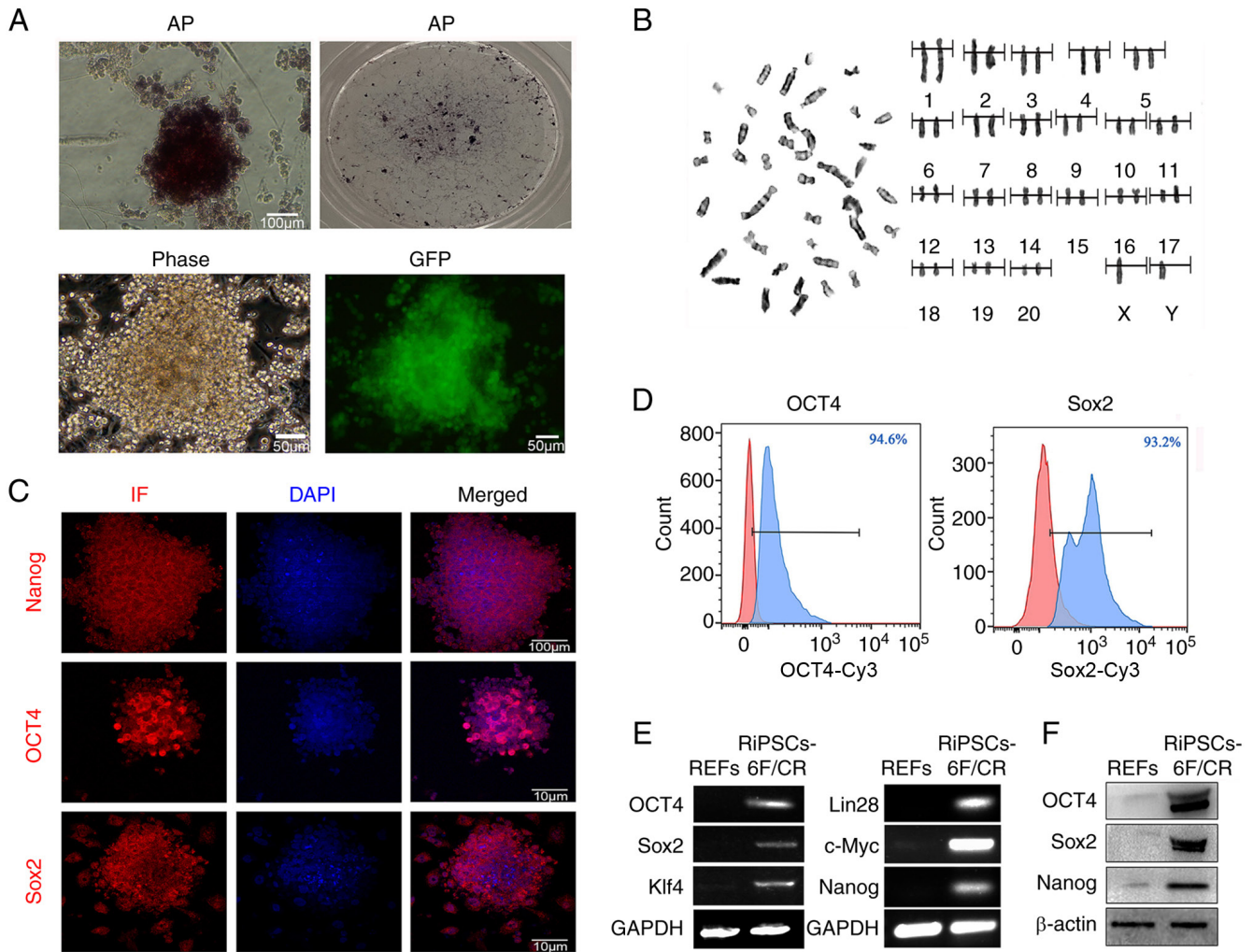


Figure 2. Biological characterization of RiPSCs-6F/CR. (A) AP-positive dense cell colonies of RiPSCs-6F/CR. (B) Chromosome G-banding analysis of RiPSCs-6F/CR. (C) RiPSCs-6F/CR expressed the pluripotency markers OCT4, Sox2 and Nanog, as observed by immunofluorescence (scale bars, 100  $\mu$ m). (D) Expression of OCT4 and Sox2 in RiPSCs-6F/CR was detected using flow cytometry. (E) Expression of six transcription factor genes was detected by reverse transcription PCR. (F) Expression of pluripotency markers was detected by western blotting. RiPSCs-6F/CR, rat induced pluripotent stem cells induced by OCT3/4, Sox2, Klf4, c-Myc, Nanog and Lin28 + CR; CR, CHIR99021 and RepSox; AP, alkaline phosphatase.

groups were performed using independent Student's t-test. For multiple comparisons, one-way ANOVA followed by Tukey's post hoc test was used to analyze the data. GraphPad Prism software 7.0 (GraphPad Software, Inc.) was used for statistical analyses and to produce the graphs.  $P < 0.05$  was considered to indicate a statistically significant difference.

## Results

**Morphological characteristics and identification of pluripotency of RiPSCs-6F/CR.** The reprogramming procedure of rat fibroblasts transduced by the six reprogramming factors (OSKMNL) as well as CR is shown in (Fig. 1A). REFs were isolated, and a substantially homogeneous population of fibroblast-like cells was obtained after subculture for 3-4 passages (Fig. 1B). All REFs could express fibroblast-specific markers CD34 and vimentin, as determined by immunofluorescence (Fig. 1C). Moreover, the fibroblast-specific genes *S100a4*, *COL1A1* and *CD34* were also highly expressed in REFs, as determined by RT-PCR analysis (Fig. 1D). However, the REFs at P3 generation did not express epithelial cell marker genes

*CDH1* and *MUC1* (Fig. 1D). Subsequently, REFs were transduced with lentiviral particles expressing OSKMNL, and the RT-PCR results confirmed that all OSKMNL genes were over-expressed after 3 days (Fig. 1E). The REFs were then cultured in the presence of the small molecules CR at day 4 and at day 8 after the initial transduction, small GFP<sup>+</sup>/iPS-like colonies could be observed. After 20 days, these GFP<sup>+</sup>/iPS-like colonies (referred to as RiPSCs-6F/CR) were picked and cultured on feeder layers for expansion and further characterization. The cell morphological changes throughout the induction process are shown in (Fig. 1F). In addition, after 20 days of treatment with empty lentiviral particles and CR, REFs showed a tendency to aggregate, but no obvious GFP<sup>+</sup> clones appeared (Fig. 1G). CR greatly increased the efficiency of generation of RiPSCs-6F/CR colonies by ~4.0-fold, resulting in 40-50 RiPSCs-6F/CR colonies from  $1 \times 10^4$  REFs within 20 days of infection (Fig. 1H). RiPSCs-6F/CR colonies showed the morphology and growth properties of embryonic stem cells (ESCs), such as typical clonal proliferation, round or oval shape, small nuclei, small cytoplasm, clear boundaries at the edges and a gradual protrusion in the center. Under an inverted

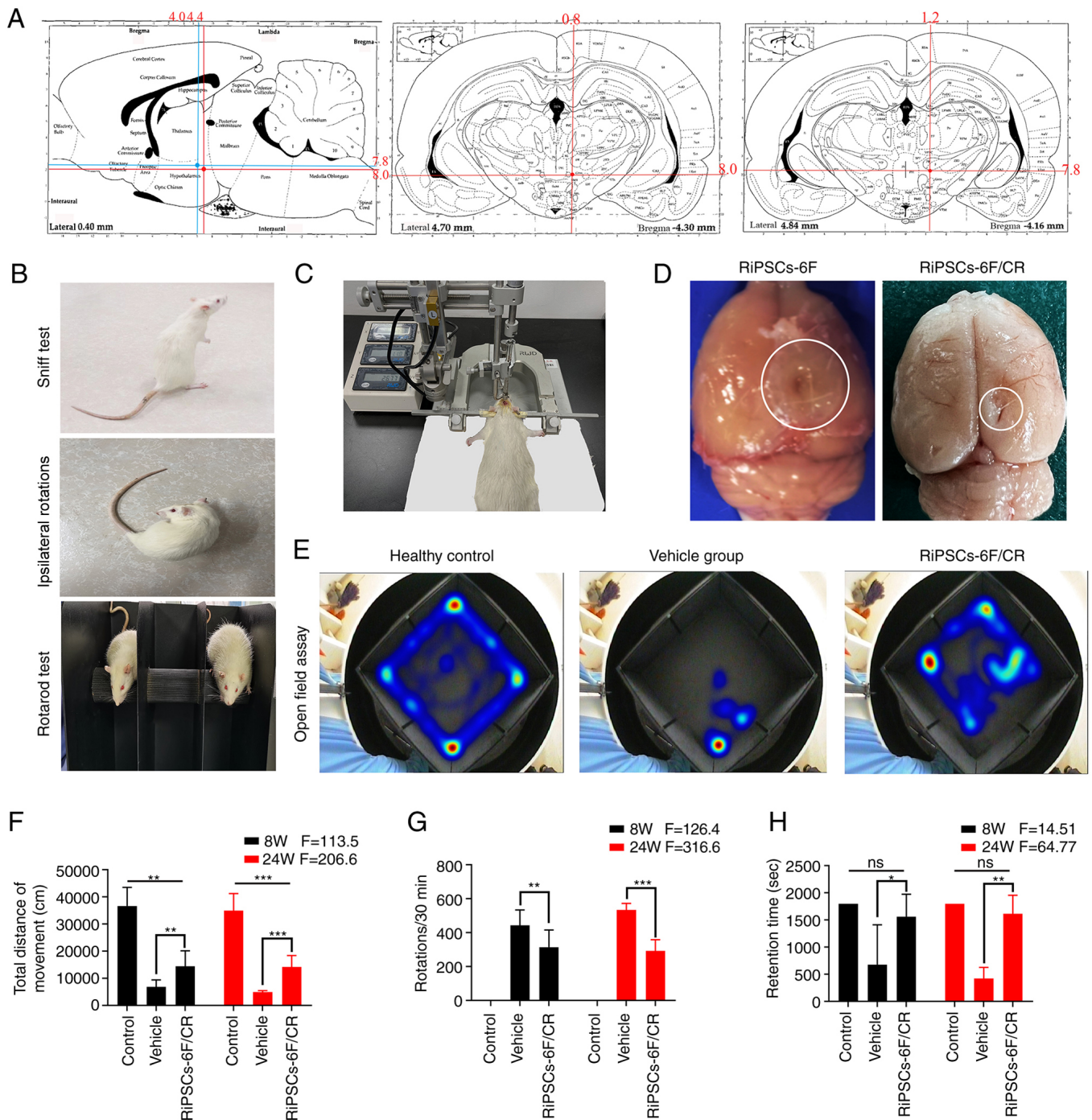


Figure 3. RiPSCs-6F/CR significantly ameliorate the behavioral deficits of a rat model of Parkinson's disease. (A) 6-Hydroxydopamine was stereotactically transplanted into the right medial forebrain bundle of each model rat at the labeled two coordinates. (B) Behavioral evaluation by sniff test, ipsilateral rotation and rotarod test. (C) Experimental rats were fixed on a stereotaxic apparatus. (D) Transplantation of RiPSCs-6F/CR did not lead to tumor formation at 8 weeks after transplantation. (E) Heat maps of open-field assay. (F-H) Motor behavior evaluation in three groups at 8 and 24 weeks after transplantation. \* $P < 0.05$ , \*\* $P < 0.01$  and \*\*\* $P < 0.001$  vs. RiPSCs-6F/CR. RiPSCs-6F, rat induced pluripotent stem cells induced by OSKMNL; RiPSCs-6F/CR, rat induced pluripotent stem cells induced by OSKMNL + CR; OSKMNL, OCT3/4, Sox2, Klf4, c-Myc, Nanog and Lin28; CR, CHIR99021 and RepSox.

microscope, it could be observed that the stereoscopic effect was strong and the cells were closely arranged (Fig. 2A).

The majority of RiPSCs-6F/CR colonies (90%) expressed high levels of AP and maintained iPS-like morphology with GFP for >25 passages (Fig. 2A). Chromosome G-banding analysis confirmed that the percentage of RiPSCs-6F/CR with normal karyotypes  $2n=42$  was 96.6%, indicating that RiPSCs-6F/CR were reproducible diploids, and there was no cross-contamination of cells from other

species (Fig. 2B). Specifically, RiPSCs-6F/CR highly expressed pluripotency-specific ESC markers, including OCT4, Sox2 and Nanog, as demonstrated by IF and flow cytometric analysis (Fig. 2C and D). RT-PCR indicated that RiPSCs-6F/CR highly expressed the six transcription factor genes (OSKMNL; Fig. 2E), and western blotting showed that RiPSCs-6F/CR also expressed numerous ESC markers at the protein level, including Sox2, OCT4 and Nanog (Fig. 2F).

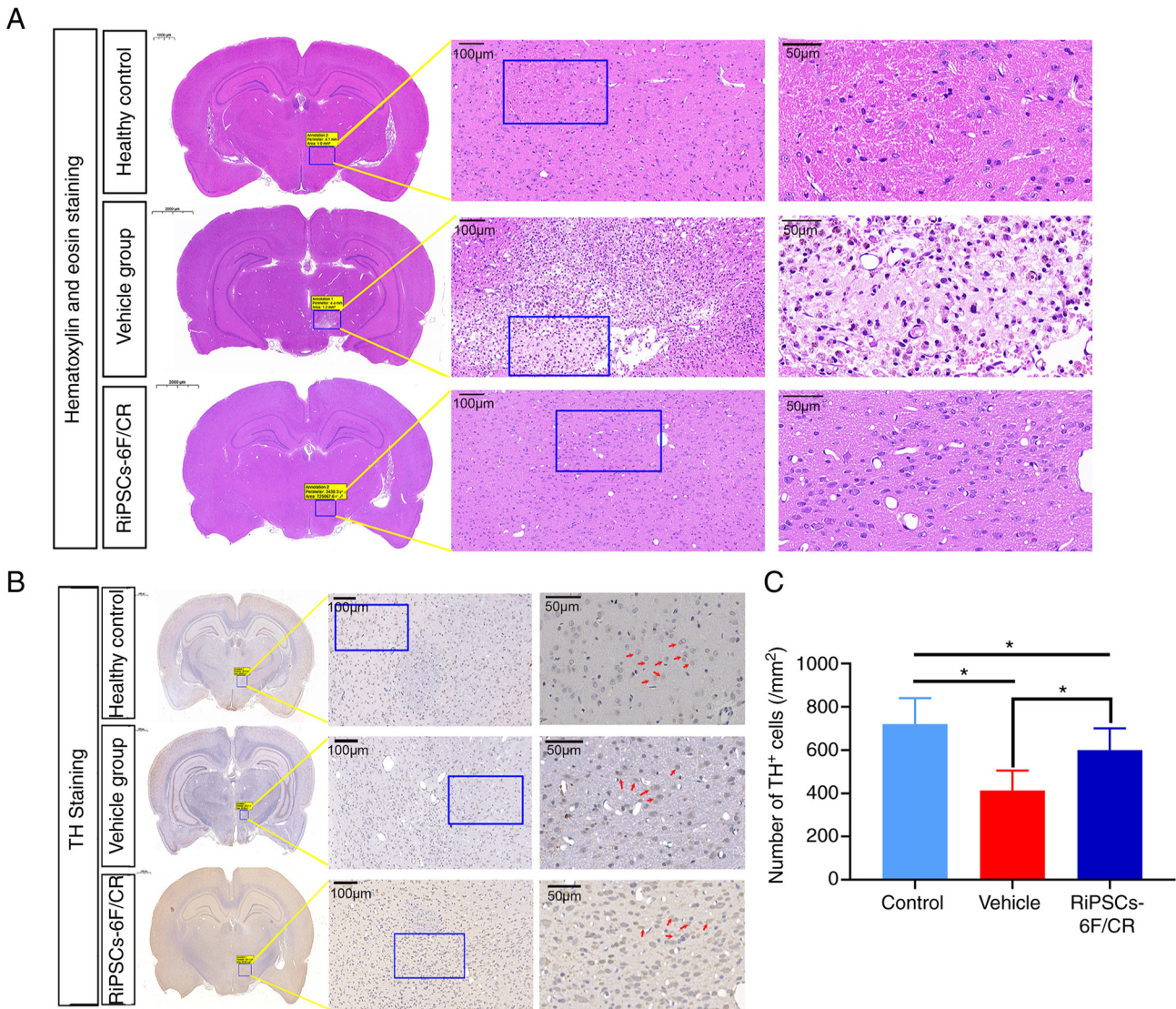


Figure 4. Effects of RiPSCs-6F/CR transplantation on the loss of TH<sup>+</sup> dopaminergic neurons in the right medial forebrain bundle of rats with Parkinson's disease. (A) Representative images of whole brain scanning with hematoxylin and eosin staining in the healthy control, vehicle and RiPSCs-6F/CR groups 12 weeks after transplantation. (B) TH intensity was detected by TH-3,3'-diaminobenzidine staining of the whole brain in three groups, and was analyzed using CaseViewer. The boxed areas are shown at higher magnification on the right side of the image. (C) Number of TH<sup>+</sup> cells in the injured areas of the three groups. \*P<0.05 by one-way ANOVA. RiPSCs-6F/CR, rat induced pluripotent stem cells induced by OCT3/4, Sox2, Klf4, c-Myc, Nanog and Lin28 + CR; CR, CHIR99021 and RepSox; TH, tyrosine hydroxylase.

*Injection of RiPSCs-6F/CR ameliorates the motor deficits of 6-OHDA-lesioned model rats with PD.* The PD rat models were prepared by stereotaxic injection of 6-OHDA into the right MFB of SD rats at two coordinates (Fig. 3A). A flow chart of the experimental procedures and animal groups described in the present study is shown in Fig. S1. At week 2 post-injection of 6-OHDA, SD rats exhibited PD-like symptoms, such as tail-pressing, back arching, sniffing and motor coordination disorder (Fig. 3B). In addition, the behavior of continuously turning >210 ipsilateral rotations/30 min to the contralateral side of the injury in APO-induced rotation was considered a main criterion for model rats with PD. A total of 30 rats were successfully modeled (83.3% success rate), as determined by a behavioral test. RiPSCs-6F/CR ( $1.0 \times 10^5$  cells/graft) were stereotactically transplanted into the right MFB of model rats with PD (n=12; Fig. 3C); all of the transplanted rats survived. In addition, transplantation

of RiPSCs-6F/CR induced by OSKMNL-CR did not lead to rejection or tumor formation (Fig. 3D). However, two out of six graft recipients of RiPSCs-6F developed tumors in the brain at 8 weeks after transplantation; therefore, all six rats in the RiPSCs-6F group were euthanized at 8 weeks due to tumorigenicity detection and no further behavioral testing was performed on the RiPSCs-6F group.

A total of 8 weeks after RiPSCs-6F/CR transplantation, the rats were more excited and active than those in the vehicle group, and the total distance of movement was significantly increased in the open-field test (P<0.01; Fig. 3E and F). In addition, the APO-induced rotation of the transplanted rats was slightly reduced at week 4 after transplantation of RiPSCs-6F/CR, but there was no significant difference compared with that of the vehicle group (n=12; data not shown). However, the APO-induced rotational behavior was significantly reduced to  $225.0 \pm 64.2$  after

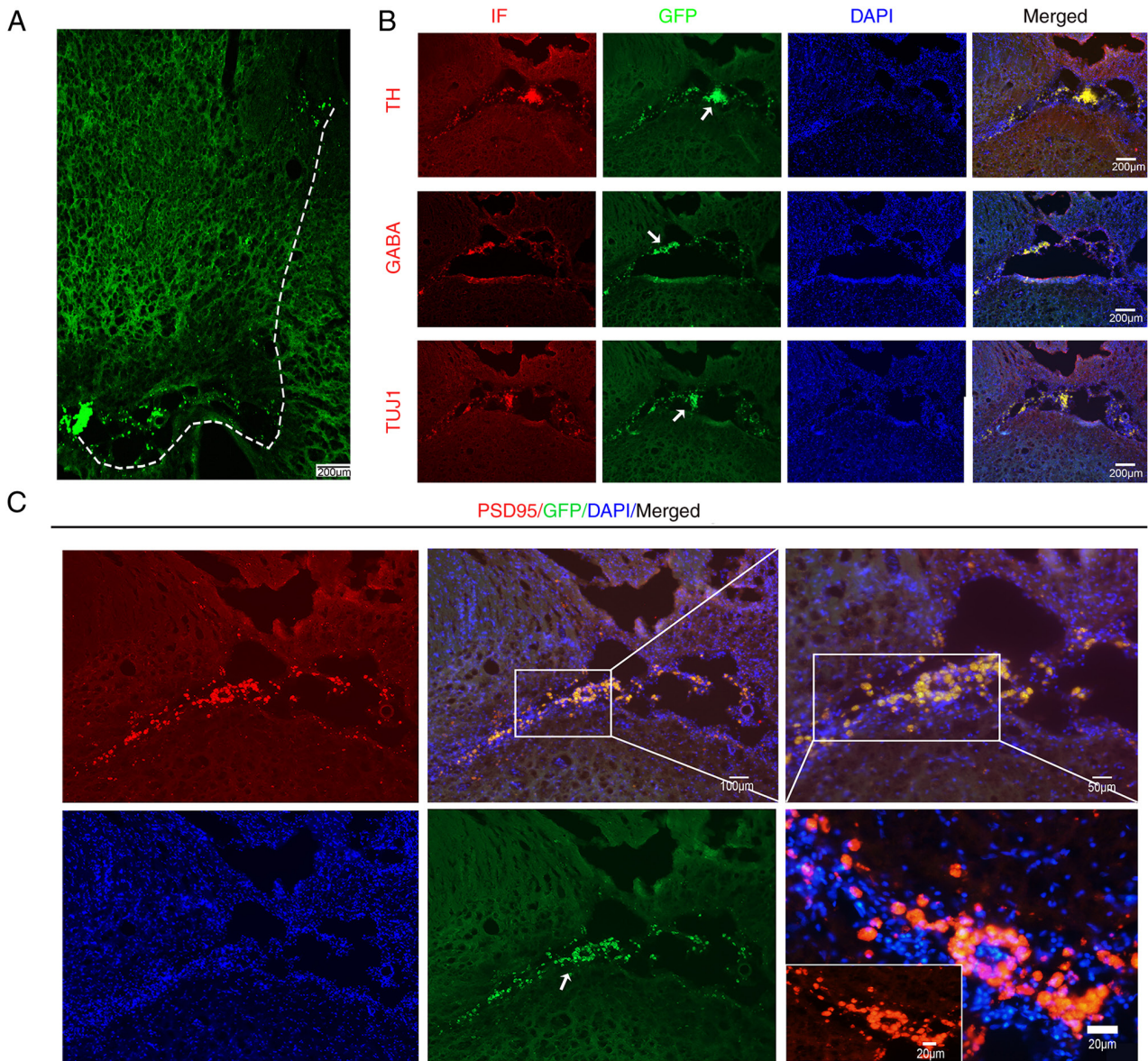


Figure 5. Survival and migration of RiPSCs-6F/CR in the right medial forebrain bundle of rats with Parkinson's disease. (A) RiPSCs-6F/CR formed a distinct graft area and migrated 2.3 mm from the graft site 20 weeks after transplantation. (B) Grafted RiPSCs-6F/CR differentiated into various functional neurons *in vivo*, which could express TH, GABA and TUJ1 20 weeks after transplantation. (C) Numerous grafted cells were positive for PSD95 staining. The transplanted RiPSCs-6F/CR were labeled by white arrows. RiPSCs-6F/CR, rat induced pluripotent stem cells induced by OCT3/4, Sox2, Klf4, c-Myc, Nanog and Lin28 + CR; CR, CHIR99021 and RepSox; TH, tyrosine hydroxylase; GABA,  $\gamma$  aminobutyric acid; TUJ1,  $\beta$ III tubulin; PSD95, postsynaptic density protein 95.

8 weeks of transplantation with RiPSCs-6F/CR ( $P < 0.01$ ; Fig. 3G). Furthermore, the motor coordination ability of the RiPSCs-6F/CR group was also effectively improved according to the results of the rotarod test ( $P < 0.05$ ; Fig. 3H). Moreover, the motor deficits of rats with PD in the RiPSCs-6F/CR group were further improved 24 weeks after cell transplantation (Fig. 3F-H), which indicated that transplanted cells required a period to induce functional recovery *in vivo*. Notably, transplantation of RiPSCs-6F/CR into the MFB may significantly improve the dyskinesia of rats with PD after 8 weeks.

*RiPSCs-6F/CR differentiate into targeted TH<sup>+</sup> dopamine neurons in the MFB of model rats with PD.* Whole-brain H&E staining analysis showed that the number of cells in the 6-OHDA-lesioned area of rats with PD was markedly lower

than that of the healthy control group, and the cells were disorderly arranged (Fig. 4A). However, numerous viable rat RiPSCs-6F/CR grafts were observed in the injured area 12 weeks after transplantation and the cells were relatively neatly arranged (Fig. 4A).

In addition, TH-DAB staining of the whole brain showed that, compared with that in the healthy control group, the number of TH<sup>+</sup> cells in the injured area of rats with PD (vehicle group) was significantly reduced, and the expression level of TH was also markedly reduced. However, numerous TH<sup>+</sup> cells were present in the grafted area of RiPSCs-6F/CR and the surrounding MFB 12 weeks after transplantation. Microscopic imaging showed markedly increased TH labeling in the transplanted MFB compared with that in the rats of the vehicle group, indicating robust recovery of the transplanted MFB from the engrafted RiPSCs-6F/CR. Moreover, stereological

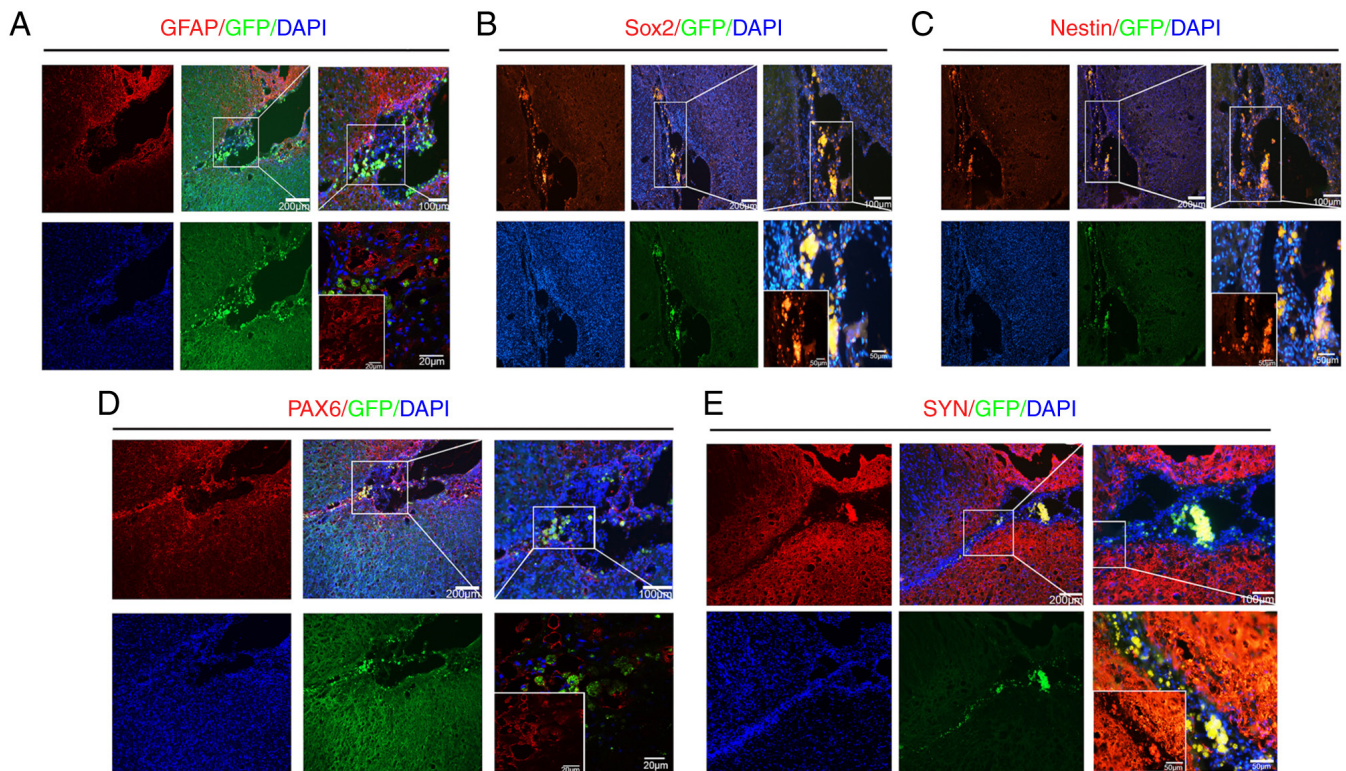


Figure 6. Differentiation and integration of RiPSCs-6F/CR cells in the brain of rats with Parkinson's disease. (A) RiPSCs-6F/CR could differentiate into GFAP<sup>+</sup> glial cells. Grafted RiPSCs-6F/CR differentiated into neural stem cells or neural precursor cells, and expressed the neural stem markers (B) Sox2, (C) Nestin and (D) PAX6 20 weeks after transplantation. (E) Approximately 52% of the transplanted RiPSCs-6F/CR cells expressed the synapse marker SYN 20 weeks after transplantation. RiPSCs-6F/CR, rat induced pluripotent stem cells induced by OCT3/4, Sox2, Klf4, c-Myc, Nanog and Lin28 + CR; CR, CHIR99021 and RepSox; GFAP, glial fibrillary acidic protein; PAX6, paired box protein 6; SYN, synaptophysin.

cell counts of TH<sup>+</sup> dopamine neurons showed that the number of viable DA neurons in the MFB of the RiPSCs-6F/CR group was significantly higher than that of the vehicle group (Fig. 4B and C). These results were in agreement with behavioral evaluations, and suggested that RiPSCs-6F/CR differentiated into targeted TH<sup>+</sup> dopamine neurons in the microenvironment of the host brain.

*RiPSCs-6F/CR differentiate into various types of functional neurons in the host MFB of rats with PD.* The results of IF detection of frozen sections of rat brain tissue showed that GFP-positive cells formed a distinct graft area 2 weeks after transplantation of RiPSCs-6F/CR. Furthermore, a large number of the transplanted cells had migrated 2.3 mm from the graft area into the surrounding brain tissue 20 weeks after transplantation (Fig. 5A). In addition, numerous GFP<sup>+</sup> cells also stained positive for TH, and certain TH<sup>+</sup> cell clusters were dispersed throughout the engraftment area and integrated into the host brain (Fig. 5B). Since TH is a specific marker of DA neurons, this suggested that RiPSCs-6F/CR could differentiate into DA neurons *in vivo*. Moreover, the engrafted RiPSCs-6F/CR gave rise to various functional neurons around and within the graft area, which could express the neuronal marker TUJ1, the GABAergic neuron marker GABA (Fig. 5B), the glutamatergic neuronal marker PSD95 (Fig. 5C) and the glial marker GFAP (Fig. 6A).

Certain GFP-positive cells exhibited features of neural stem cells or neural precursor cells, and expressed the neural stem cell markers PAX6, Sox2 and Nestin 20 weeks after transplantation (Fig. 6B-D). This indicated that the transplanted

RiPSCs-6F/CR differentiated into neural precursor cells first and then into mature neurons in the brain microenvironment. In addition, the expression of SYN was markedly increased after RiPSCs-6F/CR transplantation, and 52% of GFP<sup>+</sup> cells were also positive for SYN staining (Fig. 6E). Moreover, numerous SYN<sup>+</sup>, GFP<sup>+</sup> patches were adjacent to the transplanted RiPSCs-6F/CR, indicating that host brain-derived presynaptic terminals connected with RiPSCs-6F/CR-derived neurons to form mature synapses (Fig. 6E). These data suggested that RiPSCs-6F/CR could differentiate into neural precursor cells, various types of specific functional astrocytes and neurons in the microenvironment of the host brain. Notably, no tumor formation was found in the 12 grafted rats 20 weeks after RiPSCs-6F/CR transplantation.

## Discussion

The identification of a method capable of obtaining functional cell types is currently the most basic scientific issue in regenerative medicine research. Direct reprogramming has emerged as a promising approach to induce cell fate transition by introducing a combination of specific transcription factors (40). Moreover, previous reports have demonstrated that reprogramming efficiency could be significantly improved, and different functional cell types could be generated by the presence of certain small molecules, such as valproic acid [VPA, a histone deacetylase (HDAC) inhibitor], CHIR99021 [a glycogen synthase kinase-3 $\beta$  (GSK3- $\beta$ ) inhibitor], butyrate (an HDAC inhibitor), AZA (a DNA

methyltransferase inhibitor) and vitamin C (41,42). Moreover, PSCs could be directly induced from mouse somatic cells using a cocktail of seven small-molecule compounds called VC6TFAE (namely, VPA, CHIR99021, 616452, tranylcypromine, forskolin, AM580 and EPZ004777). Chemical reprogramming provides an alternative to the manipulation of cell fate and avoids the risk of genomic integration of exogenous transcriptional factors (43). In the present study, the small molecules RepSox (TGF $\beta$  receptor-1 inhibitor) and CHIR99021 promoted reprogramming and greatly improved the efficiency of RiPSCs-6F/CR colony generation by ~4.0-fold; notably, 40-50 iPSC colonies were generated from  $1 \times 10^4$  REFs within 25 days of infection.

Numerous studies have shown that inhibition of GSK3- $\beta$  by CHIR99021 or inhibition of TGF- $\beta$  signaling by RepSox can effectively replace Sox2 and c-Myc for reprogramming by inducing Nanog (41,43). In addition, GSK3 $\beta$  is a master regulator of Myc threonine 58 phosphorylation and leads to ubiquitin-dependent degradation of c-Myc. Therefore, inhibition of GSK3- $\beta$  by Wnt signaling could promote self-renewal and cell reprogramming by regulating the stability of c-Myc (40,44). Inhibition of TGF- $\beta$  could induce mesenchymal to epithelial transition (MET) and increase Nanog expression (36). Together with the present findings, it may be concluded that CR could promote the reprogramming process by simultaneously inhibiting GSK3- $\beta$  and TGF- $\beta$  signaling. Furthermore, the resulting RiPSCs-6F/CR had typical iPSCs-like morphology, retained normal karyotypes and AP activity, and stained positively for pluripotency-specific markers, including Nanog, OCT4 and Sox2, which shared similar characteristics with 4F-iPSCs (iPSCs induced by OCT4, Klf4, Sox2 and c-Myc) and rat ESCs (45).

ESCs and iPSCs can improve the motor behavioral defects of 6-OHDA-lesioned rats by re-innervating the striatum and restoring DA neurotransmission, but are also associated with the risk of tumor formation and teratomas *in vivo*, as well the possibility of undifferentiated cells or proliferating non-neural cells being present in the cell population (46-49). To address these issues, the use of various functional midbrain dopamine neurons and NPCs derived from iPSCs has the potential for the treatment of neurodegenerative diseases due to the lower immune rejection, lower tumorigenicity and better stability associated with these cells (50-56).

In the present study, induced RiPSCs were directly transplanted into the MFB of rats with PD. After 20 weeks of transplantation, the RiPSCs-6F/CR could form a distinct engraftment area in the MFB of rats with PD. In addition, RiPSCs-6F/CR grafts could differentiate into multiple types of functional active neurocytes and glial cells to promote behavioral recovery of motor dysfunction and neurological function of rats with PD, such as GFAP<sup>+</sup>, PSD95<sup>+</sup>, PAX6<sup>+</sup>, GABA<sup>+</sup> and TH<sup>+</sup> cells. TH serves a key role in the regulation of DA biosynthesis in DA neurons (3). A sufficient number of surviving TH<sup>+</sup> cells (DA neurons) derived from RiPSCs-6F/CR was indicated to serve an important role in behavioral improvement in the current study. In addition, GABA<sup>+</sup> cells (GABAergic neurons) derived from the RiPSCs-GFP may be responsible for regulating the balance of excitatory and inhibitory signals in the dopamine pathway. In addition, synapse formation between donor- and host-derived neurons could promote functional

recovery and behavioral improvement. Notably, no tumor formation was observed in any of the transplanted rats within 20 weeks of RiPSCs-6F/CR transplantation; however, two out of six graft recipients of RiPSCs-6F developed tumors at 8 weeks after transplantation. This result may suggest that not all iPSCs will result in tumorigenesis after transplantation *in vivo*. It may also be due to the fact that the small molecules CR facilitate reprogramming, and reduce the tumorigenicity of iPSCs *in vivo*; however, the specific mechanism needs to be further investigated (57,58). It is known that inhibition of GSK3- $\beta$  by CHIR99021 can result in activation of  $\beta$ -catenin/c-Jun signaling and downregulation of NF- $\kappa$ B activity to promote apoptosis and inhibit proliferation (59). In addition, inhibition of TGF- $\beta$  signaling by RepSox can induce MET and inhibit epithelial to mesenchymal transition, thereby inhibiting cell cycle progression and tumorigenesis (36). Small molecules are non-integrative to the genome, and are thus much safer and more advantageous than the gene editing method in modulating cell function and cell fate changes (60). Since the transplanted cells migrated in the microenvironment of the host brain, the percentage of survival and the potential mitotic activity of RiPSCs-6F/CR after transplantation needs to be further investigated.

In conclusion, in the present study, the small molecules CR significantly facilitated reprogramming and promoted RiPSCs-6F/CR colony generation during lentivirus-mediated reprogramming of six transcription factors in REFs. Furthermore, the transplanted RiPSCs-6F/CR could survive for  $\geq 20$  weeks in the MFB and could differentiate into multiple functional neurocytes to ameliorate neurological deficits in 6-OHDA-injured rats with PD.

#### Acknowledgements

Not applicable.

#### Funding

This research was supported by the National Natural Science Foundation of China (grant no. 81771381), the Anhui Provincial Key Research and Development Project (grant nos. 2022e07020030 and 2022e07020032), the Science Research Project of Bengbu Medical College (grant no. 2021byfy002), the Natural Science Foundation of the Higher Education Institutions of Anhui Province (grant nos. KJ2021ZD0085, KJ2021A0774 and KJ2021A0784), the Postgraduate Innovative Training Program of Bengbu Medical College (grant no. Byycx21048) and the Undergraduate Innovative Training Program of China (grant nos. 202110367043, 202110367044 and 20210367058).

#### Availability of data and materials

The datasets used and/or analyzed during the current study are available from the corresponding author on reasonable request.

#### Authors' contributions

JX, YL and HZ constructed the reprogramming system and drafted the manuscript, and made an equal contribution to this

work. WW and YL established the Parkinson's disease model. WG and YG participated in the statistical analysis. CM and CL conceived the research, and participated in its design and coordination. CM and CL confirm the authenticity of all the raw data. All authors read and approved the final manuscript.

### Ethics approval and consent to participate

All experimental animal procedures were approved by the Institutional Animal Care and Use Committee of Bengbu Medical college (approval no. 2020-025).

### Patient consent for publication

Not applicable.

### Competing interests

The authors declare that they have no competing interests.

### References

- Guo Y, Guan Y, Zhu H, Sun T, Wang Y, Huang Y, Ma C, Emery R, Guan W, Wang C and Liu C: Therapeutic function of iPSCs-derived primitive neuroepithelial cells in a rat model of Parkinson's disease. *Neurochem Int* 155: 105324, 2022.
- Tang Y, Meng L, Wan CM, Liu ZH, Liao WH, Yan XX, Wang XY, Tang BS and Guo JF: Identifying the presence of Parkinson's disease using low-frequency fluctuations in BOLD signals. *Neurosci Lett* 645: 1-6, 2017.
- Parmar M, Grealish S and Henchcliffe C: The future of stem cell therapies for Parkinson disease. *Nat Rev Neurosci* 21: 103-115, 2020.
- Armstrong MJ and Okun MS: Diagnosis and treatment of Parkinson disease: A review. *JAMA* 323: 548-560, 2020.
- Blesa J and Przedborski S: Parkinson's disease: Animal models and dopaminergic cell vulnerability. *Front Neuroanat* 8: 155, 2014.
- Burke RE, Cadet JL, Kent JD, Karanas AL and Jackson-Lewis V: An assessment of the validity of densitometric measures of striatal tyrosine hydroxylase-positive fibers: Relationship to apomorphine-induced rotations in 6-hydroxydopamine lesioned rats. *J Neurosci Methods* 35: 63-73, 1990.
- Bergman H, Wichmann T and DeLong MR: Reversal of experimental parkinsonism by lesions of the subthalamic nucleus. *Science* 249: 1436-1438, 1990.
- Poewe W, Seppi K, Tanner CM, Halliday GM, Brundin P, Volkman J, Schrag AE and Lang AE: Parkinson disease. *Nat Rev Dis Primers* 3: 17013, 2017.
- Limousin P and Foltynie T: Long-term outcomes of deep brain stimulation in Parkinson disease. *Nat Rev Neurol* 15: 234-242, 2019.
- Hitti FL, Ramayya AG, McShane BJ, Yang AI, Vaughan KA and Baltuch GH: Long-term outcomes following deep brain stimulation for Parkinson's disease. *J Neurosurg*: Jan 18, 2019 (Epub ahead of print).
- Karl JA, Ouyang B, Colletta K and Verhagen Metman L: Long-term satisfaction and Patient-centered outcomes of deep brain stimulation in Parkinson's disease. *Brain Sci* 8: 60, 2018.
- Liu Z and Cheung HH: Stem cell-based therapies for Parkinson disease. *Int J Mol Sci* 21: 8060, 2020.
- Pan T, Xu J and Zhu Y: Self-renewal molecular mechanisms of colorectal cancer stem cells. *Int J Mol Med* 39: 9-20, 2017.
- Takahashi K, Tanabe K, Ohnuki M, Narita M, Ichisaka T, Tomoda K and Yamanaka S: Induction of pluripotent stem cells from adult human fibroblasts by defined factors. *Cell* 131: 861-872, 2007.
- Aoi T: 10th anniversary of iPS cells: The challenges that lie ahead. *J Biochem* 160: 121-129, 2016.
- Sonntag KC, Song B, Lee N, Jung JH, Cha Y, Leblanc P, Neff C, Kong SW, Carter BS, Schweitzer J and Kim KS: Pluripotent stem cell-based therapy for Parkinson's disease: Current status and future prospects. *Prog Neurobiol* 168: 1-20, 2018.
- de Lau LM and Breteler MM: Epidemiology of Parkinson's disease. *Lancet Neurol* 5: 525-535, 2006.
- Takahashi K and Yamanaka S: Induction of pluripotent stem cells from mouse embryonic and adult fibroblast cultures by defined factors. *Cell* 126: 663-676, 2006.
- Yu J, Vodyanik MA, Smuga-Otto K, Antosiewicz-Bourget J, Frane JL, Tian S, Nie J, Jonsdottir GA, Ruotti V, Stewart R, *et al*: Induced pluripotent stem cell lines derived from human somatic cells. *Science* 318: 1917-1920, 2007.
- Chhabra A: Inherent immunogenicity or lack thereof of pluripotent stem cells: Implications for cell replacement therapy. *Front Immunol* 8: 993, 2017.
- Tiscornia G, Vivas EL and Izpisua Belmonte JC: Diseases in a dish: Modeling human genetic disorders using induced pluripotent cells. *Nat Med* 17: 1570-1576, 2011.
- Singh VK, Kalsan M, Kumar N, Saini A and Chandra R: Induced pluripotent stem cells: Applications in regenerative medicine, disease modeling, and drug discovery. *Front Cell Dev Biol* 3: 2, 2015.
- Brevini TA, Pennarossa G, Manzoni EF, Gandolfi CE, Zenobi A and Gandolfi F: The quest for an effective and safe personalized cell therapy using epigenetic tools. *Clin Epigenetics* 8: 119, 2016.
- Kim J, Jeon J, Song B, Lee N, Ko S, Cha Y, Leblanc P, Seo H and Kim KS: Spotting-based differentiation of functional dopaminergic progenitors from human pluripotent stem cells. *Nat Protoc* 17: 890-909, 2022.
- Samata B, Doi D, Nishimura K, Kikuchi T, Watanabe A, Sakamoto Y, Kakuta J, Ono Y and Takahashi J: Purification of functional human ES and iPSC-derived midbrain dopaminergic progenitors using LRTM1. *Nat Commun* 7: 13097, 2016.
- Song B, Cha Y, Ko S, Jeon J, Lee N, Seo H, Park KJ, Lee IH, Lopes C, Feitosa M, *et al*: Human autologous iPSC-derived dopaminergic progenitors restore motor function in Parkinson's disease models. *J Clin Invest* 130: 904-920, 2020.
- Kikuchi T, Morizane A, Doi D, Magotani H, Onoe H, Hayashi T, Mizuma H, Takara S, Takahashi R, Inoue H, *et al*: Human iPS cell-derived dopaminergic neurons function in a primate Parkinson's disease model. *Nature* 548: 592-596, 2017.
- Hallett PJ, Deleidi M, Astradsson A, Smith GA, Cooper O, Osborn TM, Sundberg M, Moore MA, Perez-Torres E, Brownell AL, *et al*: Successful function of autologous iPSC-derived dopamine neurons following transplantation in a non-human primate model of Parkinson's disease. *Cell Stem Cell* 16: 269-274, 2015.
- Guo Y, Zhu H, Li X, Ma C, Sun T, Wang Y, Wang C, Guan W and Liu C: Multiple functions of reversine on the biological characteristics of sheep fibroblasts. *Sci Rep* 11: 12365, 2021.
- Shenoy S: CDH1 (E-Cadherin) mutation and gastric cancer: Genetics, molecular mechanisms and guidelines for management. *Cancer Manag Res* 11: 10477-10486, 2019.
- Li M, Wang J, Wang C, Xia L, Xu J, Xie X and Lu W: Microenvironment remodeled by tumor and stromal cells elevates fibroblast-derived COL1A1 and facilitates ovarian cancer metastasis. *Exp Cell Res* 394: 112153, 2020.
- Foot O, Hallin M, Bague S, Jones RL and Thway K: Superficial CD34-positive fibroblastic tumor. *Int J Surg Pathol* 28: 879-881, 2020.
- Zarei R, Nikpour P, Rashidi B, Eskandari N and Aboutorabi R: Evaluation of Mucl Gene expression at the time of implantation in diabetic rat models treated with insulin, metformin and pioglitazone in the normal cycle and ovulation induction cycle. *Int J Fertil Steril* 14: 218-222, 2020.
- Vakhrusheva A, Endzhievskaya S, Zhuikov V, Nekrasova T, Parshina E, Ovsianikova N, Popov V, Bagrov D, Minin AA and Sokolova OS: The role of vimentin in directional migration of rat fibroblasts. *Cytoskeleton (Hoboken)* 76: 467-476, 2019.
- Jia M, Qiu H, Lin L, Zhang S, Li D and Jin D: Inhibition of PI3K/AKT/mTOR signalling pathway activates autophagy and suppresses peritoneal fibrosis in the process of peritoneal dialysis. *Front Physiol* 13: 778479, 2022.
- Guo Y, Zhu H, Li X, Ma C, Li Y, Sun T, Wang Y, Wang C, Guan W and Liu C: RepSox effectively promotes the induced differentiation of sheep fibroblasts into adipocytes via the inhibition of the TGFβ1/Smad pathway. *Int J Mol Med* 48: 148, 2021.
- Yang Y, Wang QQ, Bozinov O, Xu RX, Sun YL and Wang SS: GSK3 inhibitor CHIR99021 enriches glioma stemlike cells. *Oncol Rep* 43: 1479-1490, 2020.
- Li X, Guo Y, Yao Y, Hua J, Ma Y, Liu C and Guan W: Reversine increases the plasticity of long-term cryopreserved fibroblasts to multipotent progenitor cells through activation of Oct4. *Int J Biol Sci* 12: 53-62, 2016.

39. Casarrubea M, Sorbera F and Crescimanno G: Structure of rat behavior in hole-board: II) multivariate analysis of modifications induced by diazepam. *Physiol Behavior* 96: 683-692, 2009.
40. Li X, Zuo X, Jing J, Ma Y, Wang J, Liu D, Zhu J, Du X, Xiong L, Du Y, *et al*: Small-molecule-driven direct reprogramming of mouse fibroblasts into functional neurons. *Cell Stem Cell* 17: 195-203, 2015.
41. Li Y, Zhang Q, Yin X, Yang W, Du Y, Hou P, Ge J, Liu C, Zhang W, Zhang X, *et al*: Generation of iPSCs from mouse fibroblasts with a single gene, Oct4, and small molecules. *Cell Res* 21: 196-204, 2011.
42. Cao N, Huang Y, Zheng J, Spencer CI, Zhang Y, Fu JD, Nie B, Xie M, Zhang M, Wang H, *et al*: Conversion of human fibroblasts into functional cardiomyocytes by small molecules. *Science* 352: 1216-1220, 2016.
43. Ma Y, Xie H, Du X, Wang L, Jin X, Zhang Q, Han Y, Sun S, Wang L, Li X, *et al*: In vivo chemical reprogramming of astrocytes into neurons. *Cell Discov* 7: 12, 2021.
44. Cartwright P, McLean C, Sheppard A, Rivett D, Jones K and Dalton S: LIF/STAT3 controls ES cell self-renewal and pluripotency by a Myc-dependent mechanism. *Development* 132: 885-896, 2005.
45. Liao J, Cui C, Chen S, Ren J, Chen J, Gao Y, Li H, Jia N, Cheng L, Xiao H and Xiao L: Generation of induced pluripotent stem cell lines from adult rat cells. *Cell Stem Cell* 4: 11-15, 2009.
46. Hirabayashi M and Hoshi S: Embryonic stem (ES) cells and induced pluripotent stem (iPS) cells in rats. *Reprod Med Biol* 10: 231-238, 2011.
47. Yasuda S, Kusakawa S, Kuroda T, Miura T, Tano K, Takada N, Matsuyama S, Matsuyama A, Nasu M, Umezawa A, *et al*: Tumorigenicity-associated characteristics of human iPS cell lines. *PLoS One* 13: e0205022, 2018.
48. Fong CY, Gauthaman K and Bongso A: Teratomas from pluripotent stem cells: A clinical hurdle. *J Cell Biochem* 111: 769-781, 2010.
49. Doi D, Morizane A, Kikuchi T, Onoe H, Hayashi T, Kawasaki T, Motono M, Sasai Y, Saiki H, Gomi M, *et al*: Prolonged maturation culture favors a reduction in the tumorigenicity and the dopaminergic function of human ESC-derived neural cells in a primate model of Parkinson's disease. *Stem Cells* 30: 935-945, 2012.
50. Wei ZD and Shetty AK: Treating Parkinson's disease by astrocyte reprogramming: Progress and challenges. *Sci Adv* 7: eabg3198, 2021.
51. Duan L, Bhattacharyya BJ, Belmadani A, Pan L, Miller RJ and Kessler JA: Stem cell derived basal forebrain cholinergic neurons from Alzheimer's disease patients are more susceptible to cell death. *Mol Neurodegener* 9: 3, 2014.
52. Abdul Wahid SF, Law ZK, Ismail NA and Lai NM: Cell-based therapies for amyotrophic lateral sclerosis/motor neuron disease. *Cochrane Database Syst Rev* 12: CD011742, 2019.
53. Han F, Liu Y, Huang J, Zhang X and Wei C: Current approaches and molecular mechanisms for directly reprogramming fibroblasts into neurons and dopamine neurons. *Front Aging Neurosci* 13: 738529, 2021.
54. D'Souza GX, Rose SE, Knupp A, Nicholson DA, Keene CD and Young JE: The application of in vitro-derived human neurons in neurodegenerative disease modeling. *J Neurosci Res* 99: 124-140, 2021.
55. Ke M, Chong CM and Su H: Using induced pluripotent stem cells for modeling Parkinson's disease. *World J Stem Cells* 11: 634-649, 2019.
56. Schweitzer JS, Song B, Herrington TM, Park TY, Lee N, Ko S, Jeon J, Cha Y, Kim K, Li Q, *et al*: Personalized iPSC-derived dopamine progenitor cells for Parkinson's disease. *N Engl J Med* 382: 1926-1932, 2020.
57. Tang Y and Cheng L: Cocktail of chemical compounds robustly promoting cell reprogramming protects liver against acute injury. *Protein Cell* 8: 273-283, 2017.
58. Zhou Y, Zhu X, Dai Y, Xiong S, Wei C, Yu P, Tang Y, Wu L, Li J, Liu D, *et al*: Chemical cocktail induces hematopoietic reprogramming and expands hematopoietic stem/progenitor cells. *Adv Sci (Weinh)* 7: 1901785, 2020.
59. Lin X, Li AM, Li YH, Luo RC, Zou YJ, Liu YY, Liu C, Xie YY, Zuo S, Liu Z, *et al*: Silencing MYH9 blocks HBx-induced GSK3beta ubiquitination and degradation to inhibit tumor stemness in hepatocellular carcinoma. *Signal Transduct Target Ther* 5: 13, 2020.
60. Guan J, Wang G, Wang J, Zhang Z, Fu Y, Cheng L, Meng G, Lyu Y, Zhu J, Li Y, *et al*: Chemical reprogramming of human somatic cells to pluripotent stem cells. *Nature* 605: 325-331, 2022.



This work is licensed under a Creative Commons Attribution-NonCommercial-NoDerivatives 4.0 International (CC BY-NC-ND 4.0) License.